

# Influence of external field on spin reorientation transitions in uniaxial ferromagnets.

## I. General analysis for bulk and thin-film systems

Y. T. Millev,\* H. P. Oepen, and J. Kirschner

*Max-Planck-Institut für Mikrostrukturphysik, Weinberg 2, D-06120 Halle, Germany*

(Received 18 March 1997)

A general phenomenological discussion of spin reorientation transitions (SRT's) is given which contributes to the understanding of both bulk and thin-film behavior in applied fields. The two principal field configurations (parallel and perpendicular to the crystallographic axis of symmetry) are considered. In contrast to spontaneous SRT's, only two phases compete when an external magnetic field is applied, a canted and a field-aligned one. The complete stability analysis leads to a basic phase diagram which encompasses both configurations at once. The coexistence of phases is seen to persist even with the field and is described quantitatively. The practical implications of the analysis for temperature-driven and thickness-driven SRT's are carefully considered. [S0163-1829(98)07709-1]

### I. INTRODUCTION

The study of spin reorientation transitions (SRT's) in bulk ferromagnetic materials has a long history<sup>1-3</sup> and is still very intensive for materials involving rare-earth ions which bring about large bulk anisotropies.<sup>4</sup> Over the last few years, the phenomenon has been of increasing fundamental and technological interest in the context of thin ferromagnetic films.<sup>5</sup>

In both bulk and thin films one finds *spontaneous* reorientations in the absence of an external field. The competing effects are the different contributions to the anisotropy free energy: anisotropies of different orders and origins. In the bulk, the driving parameter for the spontaneous reorientation transitions is the *temperature*, while *thickness-driven* transitions are additionally possible in thin and ultrathin films. The strong thickness dependence of anisotropy in the latter systems originates from the characteristic contribution of interfaces. Altogether, the availability of a second tuning parameter beside temperature makes the situation with the SRT's in thin films much richer and, at the same time, much more complicated.

The application of a *magnetic field* introduces a new competitor via the unidirectional Zeeman term. The spontaneous SRT's are strongly modified and rather complicated magnetization processes may occur under variation of field. In the phenomenological treatment of homogeneous rotation of magnetization, one has to examine the free enthalpy of the system which is the sum of the anisotropy energies and the Zeeman energy. In view of the extensive literature over a long period of time, it would then seem that all features and predictions of the phenomenological approach to SRT's have by now been completely elucidated. We intend to show that this is not the case and that there are important features of the SRT's in the presence of a field which can be treated on a more general ground and can shed light on some un-noticed aspects.

A rather useful representation of the behavior of any system with anisotropy has been introduced very recently:<sup>6</sup> The anisotropy-flow concept allows one, in principle, to monitor the evolution of the system in its anisotropy space. One gains

insights into the possible generic types of reorientational behavior on very general grounds. The discussion has been carried out for spontaneous, temperature-driven SRT's in the bulk and has subsequently been generalized to the treatment of spontaneous thickness- or temperature-driven SRT's in ultrathin ferromagnetic films.<sup>7</sup> One of the purposes of this study is to show how far one can extend this anisotropy-space representation when an external field is applied to a system of *uniaxial* magnetocrystalline anisotropy. It turns out that each level of generality of treatment has its natural variables so that their choice depends on what feature one is interested in. We do not address the problem of SRT's in systems of *cubic* symmetry in an external field which has attracted more attention and has a higher symmetry of possible orientations of the easy axes;<sup>8,9</sup> we are ultimately interested in SRT's in ultrathin films where a uniaxial contribution due to the lowering of symmetry at interfaces<sup>10</sup> and/or large uniaxial strains<sup>11</sup> is typically found.

The structure of the paper is as follows. In Sec. II we present the phenomenological model for uniform rotation which encompasses very generally both bulk and thin-film systems with anisotropy of up to second order in a constant external field. To make the discussion self-contained, a brief summary of the most important features from the spontaneous (zero-field) case is given.<sup>1,2,7</sup> In addition, a short description is given for the simpler case when no higher-order anisotropy is present.<sup>12</sup>

In Sec. III we proceed with the stability analysis of the relevant free enthalpy in a most general form by identifying the natural dimensionless parameters for the two major orientations of the external field, one parallel and one perpendicular to the symmetry axis. Here, one detects for both field orientations a singular point in the relevant phase diagram which is delineated as a result of the stability analysis. In both cases, the singular point is the merging point of the curves which bound a *region of coexistence of phases*. The region has its genesis in the underlying zero-field coexistence phenomenon.

It is impossible to discuss all work related to the problem but some papers have to be mentioned here as bearing more direct relevance to the mathematical analysis involved. Ono-

prienko is the first who considered the problem in its depth.<sup>13</sup> He described in detail the in-plane configuration for bulk systems. Mitsek *et al.*<sup>14</sup> considered the singular point in greater detail and were able to detect interesting features of the astroid curve<sup>1,15</sup> which were due to the effect of higher-order anisotropy. References 16,17 also addressed third-order anisotropy in an external field (see also Refs. 18,19). Asti and Bolzoni<sup>17,19</sup> emphasized the formal transformations between the analyses for the two field orientations and determined the phase boundaries by equating the energies of the competing phases, thus implementing the so-called *Maxwell convention*.<sup>20</sup> The full-scope stability analysis, on the other hand, delineates the exact thermodynamic boundaries and thus also the regions of coexistence and metastability of phases whereby the magnetization processes are interpreted in the *perfect delay convention*.<sup>20</sup> A balanced and illuminating discussion of both approaches is given in Ref. 20. We carry out a general stability analysis for both field configurations up to anisotropy of second order. The phase line of equal depth of coexisting minima which is important within the Maxwell convention is also given. However, the magnetization processes are not in the focus of this study; rather, we lay emphasis on the representations in the anisotropy space which are especially promising and will be exploited in the context of thin films (part II, next paper).

Section IV is devoted to the specification of the phase diagrams in the more physical terms of reduced field and ratio of the first to the second anisotropy constants. The coexistence phenomenon and the singular point are seen to exist only for negative values of the second anisotropy constant. The formal symmetry of the general treatment is presented in suitable diagrams in terms of the relevant physical parameters. The ‘‘physical’’ representation leads to a certain lifting of the degeneracy of the formal description, thus revealing the important differences between coaxially and perpendicularly oriented fields.

Section V introduces a presentation in terms of the anisotropy constants scaled against the Zeeman energy amplitude. This representation seems to be particularly well suited to the investigation of thickness-driven SRT’s in thin films, since it preserves the linearity of the anisotropy flows which has been found in the case without field.<sup>7</sup>

In Sec. VI, we summarize the results and discuss prospective applications and extensions of the method.

## II. THE MODEL AND ITS RELEVANT LIMITING CASES

We examine a uniaxial system with anisotropy free energy density of the form<sup>1-3</sup>

$$f_A = a \sin^2 \theta + b \sin^4 \theta, \quad (1)$$

where  $a$  and  $b$  are the first and second anisotropy contributions, respectively, while the angle between the direction  $\mathbf{n}$  of the axis of uniaxial anisotropy and the direction of magnetization  $\mathbf{M}$  is denoted as  $\theta$  (Fig. 1). Both constants may encompass contributions other than the purely magnetocrystalline ones as, for instance, contributions due to magnetoelastic coupling.<sup>21</sup> In both bulk and thin-film systems, there may exist a dipolar (shape) anisotropy contribution to the first anisotropy constant  $a$ . This is important only for small ferromagnetic particles or when one or two of the dimen-

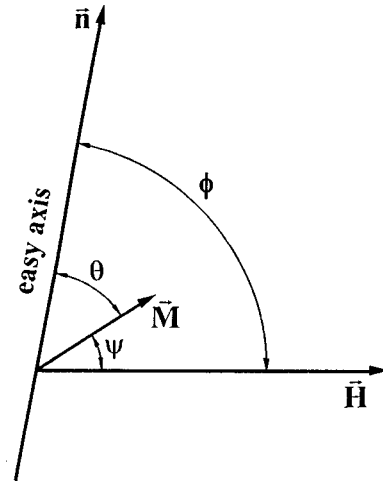


FIG. 1. The geometry of the uniaxial problem in applied magnetic field.

sions of the system are much smaller than the rest, as in thin films or needles. In any case, the dipolar contribution to the overall anisotropy plays a central role in the context of thin-film SRT’s. Anisotropies in the plane perpendicular to the axis  $\mathbf{n}$  are neglected as irrelevant to the salient features of the SRT in the corresponding system (see, however, the second to the last paragraph in the Discussion, Sec. VI).

Once a magnetic field has been applied to the system (Fig. 1), the anisotropy energetics of the system is contained in the enthalpy density<sup>1-3,20</sup>

$$g_A = f_A + \epsilon_Z, \quad (2)$$

where  $\epsilon_Z$  is the Zeeman term which favors parallel alignment of magnetic moment and external field and is thus of a *uni-directional anisotropy type*. Explicitly,

$$\epsilon_Z = -\mathbf{H} \cdot \mathbf{M} = -HM_H = -HM \cos \psi = -z \cos \psi. \quad (3)$$

Here,  $\mathbf{H}$  and  $\mathbf{M}$  denote external field and saturation magnetization, respectively,  $M_H$  is the component of magnetization along the magnetic field, while the last equation defines the quantity  $z$ . As we neglect anisotropies in the plane perpendicular to  $\mathbf{n}$ , the magnetization vector lies always in the plane determined by  $\mathbf{n}$  and  $\mathbf{H}$ . We use  $\mathbf{H}_n$  when the field is parallel to the easy axis  $\mathbf{n}$  and  $\mathbf{H}_p$  when the field is perpendicular to the easy axis. These two principal field configurations will occasionally be called *coaxial* and *in-plane*, respectively. For a general orientation of the field, the angle  $\phi$  between  $\mathbf{H}$  and  $\mathbf{n}$  and  $\theta$  are the two relevant angular variables in the problem ( $\psi$  together with any of  $\theta$  or  $\phi$  is just as good a choice; in the absence of in-plane anisotropy terms  $|\psi| = |\phi - \theta|$ ). Assuming that in practice  $\phi$  can be controlled, one remains with a minimization problem for the enthalpy as a function of  $\theta$ . This is the Stoner-Wohlfarth problem,<sup>12,15</sup> extended to include higher-order anisotropy.<sup>13,14,18</sup>

Now then, for an *arbitrary* direction of the field (i.e., for an arbitrary  $\phi$ ), even if the higher-order anisotropy  $b$  is identically zero, one has to solve a general quartic equation and study the stability of its solutions. Equivalently, one finds a parametric solution for the boundaries between stable and metastable states in the  $(H_n, H_p)$  plane which leads to the so-called astroid curve.<sup>1,15,18</sup> A geometrical (graphical) con-

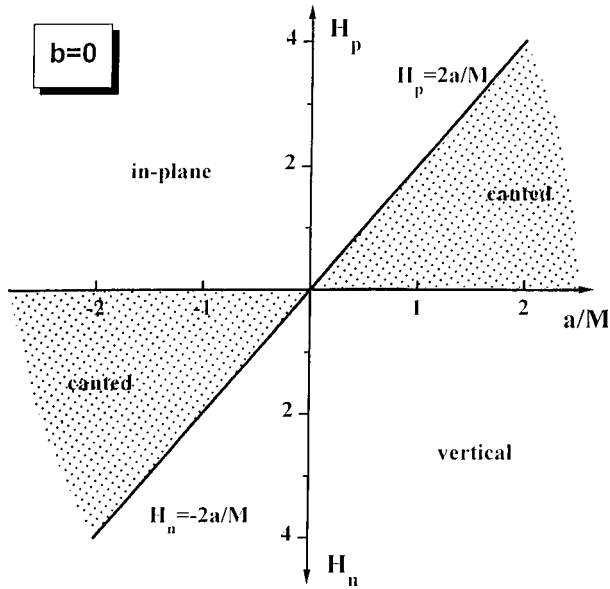


FIG. 2. Phase diagram for uniaxial ferromagnet in external field. Only first-order anisotropy contributions are considered. Both field configurations are given in one plot. Upper half-plane: in-plane field configuration ( $\mathbf{H}_p$ ); lower half-plane: coaxial field orientation ( $\mathbf{H}_n$ ). The phase boundaries occur at magnitudes of the applied field equal to the anisotropy field  $H_A = 2|a|/M$ .

struction is used to extract the equilibrium direction of magnetization and to study the processes of magnetization, due to variations of field. If  $b \neq 0$ , the minimization equation to be solved is of eighth degree, but the problem still allows an astroid type of analysis.<sup>14,18</sup> However, the relative simplicity of the picture is lost and the analysis has remained incomplete.

For the problem that we are interested in, one can always arrange to have the field fixed in a coaxial or in-plane configuration with respect to the axis  $\mathbf{n}$ . Hence, it makes sense to study separately the cases with parallel field  $\mathbf{H}_n$  and with in-plane field  $\mathbf{H}_p$ . Apart from the simplification achieved by the choice of particular directions of the field, we will only discuss solutions with  $0 \leq \theta \leq \pi/2$  ( $0 \leq \cos \theta, \sin \theta \leq 1$ ), i.e., we are not interested in magnetization processes under direction reversal of applied field in the context of this paper.

#### A. Limiting case of vanishing higher-order anisotropy

In the general analysis, it will soon turn out that the *sign of the second anisotropy constant*  $b$  is very important. In addition, normalization with respect to  $b$  will be required at certain stages. It is, therefore, advisable to sort out the simple case of  $b=0$  for the two distinct orientations of field.

With  $b=0$ , the minimization procedure is pretty transparent. One requires that  $dg_A/d\theta=0$ ,  $d^2g_A/d\theta^2 \geq 0$ . The results are summarized in Fig. 2. Note that in this figure we have found it more instructive and compact to present both field configurations in the same plot, whereby the upper (lower) half-plane refers to the in-plane (coaxial) configuration, respectively. An important feature which holds throughout the analysis with applied field is that *only two phases* of different orientations of magnetization may occur. In the two configurations we are going to consider, these are invariably a phase of magnetization collinear with the field direction (field-

aligned or conforming phase) and a phase of canted magnetization (canted phase). With or without higher-order anisotropy, a phase with the magnetization perpendicular to a field corresponds to a state of uncompensated torque acting on the magnetization which is why it cannot be sustained physically.

In the absence of higher-order anisotropy, the phase diagram in this presentation exhibits central symmetry (Fig. 2) with the projection of magnetization along the respective field direction being equal in both cases:

$$m_H = \frac{M_H}{M} = \frac{H}{H_A}, \quad (4)$$

where  $H_A = 2|a|/M$  is the so-called anisotropy field.<sup>2,3,20</sup> It is useful to think about this diagram in its connection with the underlying zero-field case, where the two possible phases (for  $b=0$ ) share equal portions of the allowed parameter space  $-\infty < a < +\infty$ : in-plane wins for negative  $a$ , coaxial wins for positive  $a$ ; the border point is simply  $a=0$ . With the field, this point gives birth to the respective borderlines in Fig. 2. Coaxial ( $\mathbf{H}_n$ ) or in-plane ( $\mathbf{H}_p$ ) field boosts the zero-field phase of the same name, while the other competitor phase is disfavored by the applied torque and is modified to a canted phase of a relatively small domain of stability. The SRT occurs between these two phases upon variation of some physical parameter such as temperature for bulk and thin-film systems or thickness for the latter. The field is assumed constant in magnitude and direction.

#### B. Limiting case of zero applied field

Similar heuristic projection onto the simpler spontaneous case is useful with the more complicated diagrams to be encountered below. When  $b \neq 0$ , the reference zero-field case is best described in the anisotropy space of the system, i.e., in the plane  $(a,b)$ .<sup>6</sup> Due to the higher-order anisotropy contribution, three stable spontaneous phases are possible, the additional one being a *spontaneously* or “true” canted phase. The coaxial phase is absolutely stable for  $a > 0$ ,  $a > -b$ , the in-plane phase is so for  $b < 0$ ,  $b < -a$ , the canted one sets in for  $a < 0$ ,  $b > -a$ . The most interesting feature is the *coexistence of phases* with easy-axis and easy-plane orientations of magnetization for  $a > 0$ ,  $b < -a/2$ . The anisotropy-flow concept allows one, in principle, to follow the trajectory of the system under variation of the driving parameter and to detect the possible SRT’s when the system crosses over to a phase of greater relative stability in the anisotropy space.<sup>6,7</sup> One of the important issues of this paper is to explain in detail how and to what extent the coexistence phenomenon projects itself onto the physical situation with an applied field, whereby a certain generalization of the anisotropy-flow concept appears both useful and inevitable.

### III. GENERAL STABILITY ANALYSIS WITH UP TO SECOND-ORDER ANISOTROPY CONTRIBUTIONS IN APPLIED FIELD

As discussed in the preceding section, the different phases are to be distinguished by the corresponding equilibrium orientations of the magnetization vector  $\mathbf{M}$ . These are to be found and classified by examining the enthalpy density

$$g_A = a \sin^2 \theta + b \sin^4 \theta - MH \cos(\theta - \phi). \quad (5)$$

The necessary condition for the existence of extrema of  $g_A(\theta)$  is

$$\frac{d}{d\theta} g_A = (a + 2b \sin^2 \theta) \sin 2\theta + MH \sin(\theta - \phi) = 0. \quad (6)$$

The sufficient condition for an extremum to be a minimum is

$$d^2 g_A / d\theta^2 \geq 0 \quad (7)$$

at the points determined by solving Eq. (6).

#### A. Magnetization parallel to the field direction (field-aligned or conforming solution)

For both coaxial ( $\phi=0$ ) and in-plane ( $\phi=\pi/2$ ) field configurations, Eq. (6) always has a solution corresponding to magnetization pointing along the applied field (field-aligned or conforming solution). Mathematically, this is seen in the factoring out of  $\sin \theta$  or  $\cos \theta$  in Eq. (6). The simple solutions bring about simple stability conditions as well. By Eq. (7), in the coaxial configuration the conforming phase is stable for

$$z + 2a \geq 0 \Rightarrow H \geq H_{A1} = -2a/M \geq 0, \quad (8)$$

while in the in-plane configuration the conforming phase is stable for

$$z - 2a - 4b \geq 0 \Rightarrow H \geq H_{A2} = (2a + 4b)/M \geq 0. \quad (9)$$

$H_{A1}$  and  $H_{A2}$  are anisotropy fields.<sup>22</sup> In contrast to the above-discussed case with a lowest-order anisotropy contribution only, one finds two different anisotropy fields for the different field configurations. As will be discussed in the next section, two distinct anisotropy fields can indeed be detected for a particular range of values of the ratio  $a/b$ .

#### B. Magnetization tilted with respect to the field direction (canted-phase solution)

The following general remarks have to be made before proceeding with the solution which corresponds to the canted phase in both configurations of field. There are *three* parameters of the dimension of energy density in Eq. (5) for the direction-dependent part of the enthalpy. These are the amplitude of the Zeeman energy  $z=HM$  and the first and second anisotropy constants  $a$  and  $b$ . From the physical point of view, only two independent ratios are relevant. This can be easily recognized in the freedom of choice to measure the enthalpy in units of any one from among  $a$ ,  $b$ , and  $z$ . Besides, one is always free to define the zero of the enthalpy via shifting by a quantity which is angle independent.<sup>23</sup>

In the following, we examine three different dimensionless pairs. The first of these, the variables  $p$  and  $q$ , allows a straightforward mathematical description for the canted-phase solution of Eq. (6) *simultaneously* for both field configurations. The second pair,  $r=a/b$  and  $\bar{H}=H/H_C$ , where  $H_C$  is a certain critical field, allows the interpretation of the mathematical results in more conventional terms, while the third pair,  $\alpha=a/HM$ ,  $\beta=b/HM$ , based on scaling against

the amplitude of the Zeeman energy, is most suitable for the extension of the anisotropy-flow concept introduced in studies on spontaneous SRT's.<sup>6,7</sup>

Let us now discuss the canted-phase solution for the *coaxial* configuration. We define dimensionless ratios  $p$  and  $q$  as follows:<sup>24</sup>

$$p = -\left(1 + \frac{a}{2b}\right), \quad q = -\frac{z}{4b} = -\frac{HM}{4b} (b \neq 0). \quad (10)$$

The inverse transformation to  $(a,b)$  for a given  $z$  is  $a=(p+1)z/2q$ ,  $b=-z/4q$ . Denoting with  $x_n$  the normalized projection of magnetization along the field  $\mathbf{H}_n$ ,  $x_n = M_n/M = \cos \theta$ , one can use the freedom in fixing the zero and the scale of energy in order to cast the angular-dependent part of the enthalpy  $g_A(\theta; p, q)$  as

$$\frac{g_A - (a+b)}{4|b|} = \text{sgn}(-q)x_n \left( q + \frac{1}{2} p x_n + \frac{1}{4} x_n^3 \right). \quad (11)$$

The extremal Eq. (6) assumes the form

$$\sin \theta \cdot (x_n^3 + p x_n + q) = 0, \quad (x_n = \cos \theta \in [0, 1]). \quad (12)$$

We have already discussed the field-aligned (conforming) solution  $\sin \theta=0$  ( $\theta=0$ ) and its stability in the previous subsection. The canted-phase solution has to be found by solving the cubic and testing for stability. The cubic is *in its reduced form* with the ratios  $p$  and  $q$  defined as above which automatically means that these are the natural parameters for the mathematical solution of the problem.<sup>25</sup>

With the in-plane configuration, the problem can be formally given precisely the same appearance by defining  $P$  and  $Q$  as

$$P = a/2b, \quad Q = -z/4b = -HM/4b. \quad (13)$$

The transformation back to  $(a,b)$  is given by  $a=-zP/2Q$ ,  $b=-z/4Q$ . Denoting with  $x_p$  the normalized projection of magnetization along the in-plane field  $\mathbf{H}_p$ ,  $x_p = M_p/M = \sin \theta$ , one finds that

$$\frac{g_A}{4|b|} = \text{sgn}(-Q)x_p \left( Q + \frac{1}{2} P x_p + \frac{1}{4} x_p^3 \right) \quad (14)$$

and this is formally the same object as in Eq. (11) above. The same is true for the appearance of the extremal equation which is now

$$\cos \theta (x_p^3 + P x_p + Q) = 0, \quad (x_p = \sin \theta \in [0, 1]). \quad (15)$$

Thus, the coaxial and in-plane configurations of the field can be discussed simultaneously, since the angular parts of the duly normalized enthalpies are identical as are the minimization equations for the magnetization components along the applied field. Moreover, the same formal identity holds for the sufficient condition for the canted-phase extremum to be a minimum. Making use of the cubic to reduce the powers of  $x$  in the condition  $d^2 g_A / d\theta^2 \geq 0$ , one finds that the canted-phase solution is stable whenever it holds true that

$$qf[p, q, x(p, q)] \leq 0, \quad (16)$$

where the function  $f(p, q)$  is given by the expression

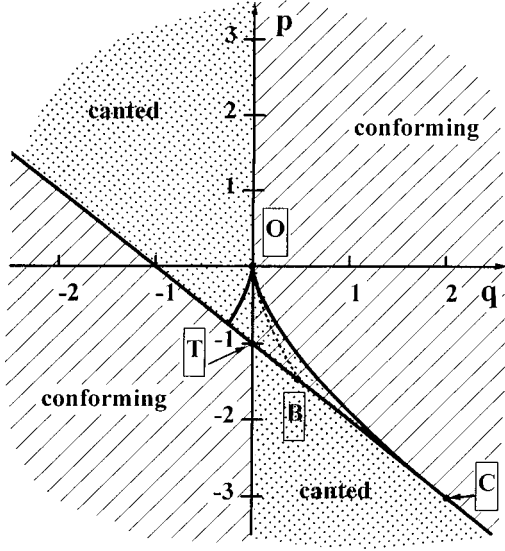


FIG. 3. Phase diagram for uniaxial ferromagnet in applied field in the  $(p, q)$  representation. The mathematically natural variables  $(p, q)$  are defined in Eqs. (10) and (13). The representation encompasses *both* field configurations. Left (right) half-plane corresponds to positive (negative) second-order anisotropy  $b$ . Coexistence of phases is only possible for negative  $b$  within the curvilinear triangle  $OCT$ ; the respective minima of the free enthalpy are of equal depth along the line  $OB$ . The straight boundaries through  $B$  and  $T$  emerge from the stability condition on the conforming phase. For  $b < 0$ , the canted phase invades the domain of the conforming phase up to the line  $OC$ . The tricritical point  $C$  is the point of tangence of  $BT$  with the curve starting at the origin. The  $p$  axis corresponds to the spontaneous (zero-field) case, whereby the segment  $OT$  represents the “true” canted phase in zero field. Besides, for given anisotropies the  $p$  axis cannot be traversed without a change to the opposite direction of the applied field.

$$f(p, q) = (2p + 3)x^2(p, q) + 3qx(p, q) + p \quad (17)$$

and it is understood that  $x(p, q)$  is the root of the cubic for the relevant field configuration.

The required information for the solutions of the cubic is given in the Appendix. We proceed with a discussion of the results of this general stability analysis.

### C. The $(p, q)$ diagram and stability of phases

Since both field configurations are reduced to the same formalism, it is sufficient to discuss in detail either the  $(p, q)$  or the  $(P, Q)$  presentation, the discussion being literally valid for the other case as well. Solving Eq. (6) and imposing the condition (16), one constructs the stability diagram, presented in Fig. 3. Only the lines which bear relevance to the anisotropy problem in question have been preserved in the plot. The straight line is given by the equation

$$p + q + 1 = 0. \quad (18)$$

The curves starting at the origin are the relevant portions of the curve, given by the equation (see the Appendix)

$$D \equiv p^3/27 + q^2/4 = 0. \quad (19)$$

Equation (18) represents the borderline of stability ( $g''_{A|x=1} = 0$ ) for the conforming phase. This line and the  $p$  axis

divide the plane  $(p, q)$  into four segments which come together at the point  $T(p = -1, q = 0)$ . Unlike the zero-field case, in applied field only two phases are possible, the conforming and the canted one. Mathematically, this is seen in the fact that as soon as the Zeeman terms in Eqs. (12) and (15) are nonzero, one cannot factor out an additional trigonometric function ( $\sin \theta$  or  $\cos \theta$ ) and these are the ones that bring about the third possible phase. The conforming solution (magnetization along the field) is stable in the two larger segments which appear shaded in Fig. 3. The canted-phase solution is stable in the remaining two smaller segments. The different regions of the two phases are connected via the point  $T$ . Additionally, the canted phase is stable within the curvilinear triangle  $OCT$  which belongs also to the larger segment on the right-hand side. In other words, *within this triangle both canted and conforming phases coexist*. Analytically, the triangle is described by the conditions

$$-3 \leq p \leq 0, \quad (20)$$

$$\max(0, -p - 1) \leq q \leq \sqrt{-27p^3/4}. \quad (21)$$

Here, the competing phases correspond to two distinct local minima of the enthalpy  $g_A$ . One of these minima is always deeper except along the line of exchange of stability defined by the condition  $g_A(\text{canted}) = g_A(\text{conforming})$ . Explicitly, the line of equal depth for both minima (dotted line  $OB$  in Fig. 3) is given by

$$p = -\frac{3}{2^{1/3}}q^{2/3} \quad \text{for } q \in \left[0, \frac{1}{2}\right]. \quad (22)$$

Along  $OB$  the conforming and the canted phase exchange stability. It corresponds to the Maxwell-convention borderline<sup>20</sup>: in this scenario, the transition between the two phases takes place when both minima are equally deep, i.e., along the line  $OB$  (examples are given in Ref. 20). Metastability effects due to “overheating” or “undercooling” are not expected. The other alternative, the perfect-delay convention,<sup>20</sup> suggests that under variation of the driving parameter the system is trapped in the minimum from which it started its evolution. It remains there until the minimum disappears completely.<sup>7,20</sup> No switching to the deeper minimum of the competing phase occurs within the region of coexistence. The canted-phase solution of the cubic is  $x_3(p, q)$  which is the relevant one from among three real solutions available in this region (see the Appendix). In between the two minima there must be a local maximum. The maximal solution of the cubic is  $x_2(p, q)$  (see the Appendix). This solution is important if the height of the barrier separating the two local minima is required.

In view of the definition of  $q = Q = -z/4b$  with  $z > 0$  and the fact that one finds coexistence for  $q$  or  $Q$  positive, it follows immediately that *coexistence is only possible for negative values of the second anisotropy constant*. Point  $C$  is perhaps the most interesting point in the phase diagram. More precisely,  $C$  is the merging point of the line  $D(p, q) = 0$  of discontinuous transitions<sup>13</sup> with the line  $p + q + 1 = 0$  of continuous reorientation transitions, hence, it can be interpreted as a *tricritical point* (more generally, as a multicritical point) in the sense of the theory of phase transitions and critical phenomena.<sup>1</sup>

#### IV. SPECIFICATION OF THE PHASE DIAGRAMS FOR BOTH FIELD CONFIGURATIONS IN PHYSICAL TERMS

In this chapter, we deduce the field–anisotropy diagrams in the form of two-dimensional plots for both field orientations studied. The translation of the general mathematical results presented in Fig. 3 is formally effected by the inverse transformations to the anisotropy variables. They have been given above.

The existence of the critical point  $C$  in the  $(p, q)$  diagram provides the opportunity for a suitable physical scaling of the quantities involved. Since  $q_{cr}(Q_{cr}) = 2$ , one finds that in both field configurations the critical field  $H_C$  is given by<sup>13,14,18</sup>

$$H_C = 8|b|/M, \quad (23)$$

while, with  $p_{cr}(P_{cr}) = -3$ , the relation between the first and second anisotropy constants at the critical point is  $a = 4b$  ( $b < 0$ ) for the coaxial configuration and  $a = -6b$  ( $b < 0$ ) for the in-plane configuration. The results can be suitably presented on a single diagram for both field configurations in close correspondence with the choice of axes in Fig. 2. In Fig. 4(a) one finds the diagram for positive second anisotropy constant ( $b > 0$ ), while Fig. 4(b) presents the case with negative  $b$ . The proper units are  $\bar{H}_n \equiv H_n/H_C = H_n M/8|b|$  or  $\bar{H}_p \equiv H_p/H_C = H_p M/8|b|$  for the ordinate axes and  $r \equiv a/b$  for the abscissa. The upper parts of both diagrams refer to the in-plane field configuration, the lower ones concern the coaxial configuration. Due to the effect of higher-order anisotropy, the diagrams are substantially different from that of Fig. 2. The general feature which is preserved from the  $b = 0$  case of Fig. 2 is that the conforming phases dominate the larger portions of the diagram, while the canted phase occupies much smaller areas. Besides, this presentation preserves the formal central symmetry of the diagrams for each of the signs of  $b$ ; the center of symmetry, however, is shifted to  $r = -1$ . Thus, the very presence of higher-order anisotropy modifies significantly the structure of the phase diagram.

##### A. Positive higher-order anisotropy [ $b > 0$ , Fig. 4(a)]

In the coaxial configuration [lower part of Fig. 4(a)], the borderline between conforming and canted phases is given by  $\bar{H}_n = -r/4$  and thus traverses the origin. In the in-plane configuration [upper part of Fig. 4(a)], the borderline is given by  $\bar{H}_p = (2+r)/4$ . If  $H_n = H_p = 0$ , the diagram collapses onto the abscissa which describes the case of spontaneous SRT's ( $H = 0$ ): in-plane for  $0 < b < -a/2$ , canted with  $b > -a/2 > 0$ , and coaxial for  $a > 0$ ,  $b > 0$ . It is only along the abscissa (zero field) that a monotonic anisotropy flow driven by thickness, temperature, or some other parameter would traverse *two* border points. As soon as the field is applied and as long as the second constant  $b$  is positive, any monotonic trajectory cannot have more than one cross point in a given field configuration. Hence, peculiarities are to be expected only at a unique point in the phase diagram for a fixed field configuration. In other words, each of the spontaneous cross points gives rise to a single phase borderline in the corresponding field configuration.

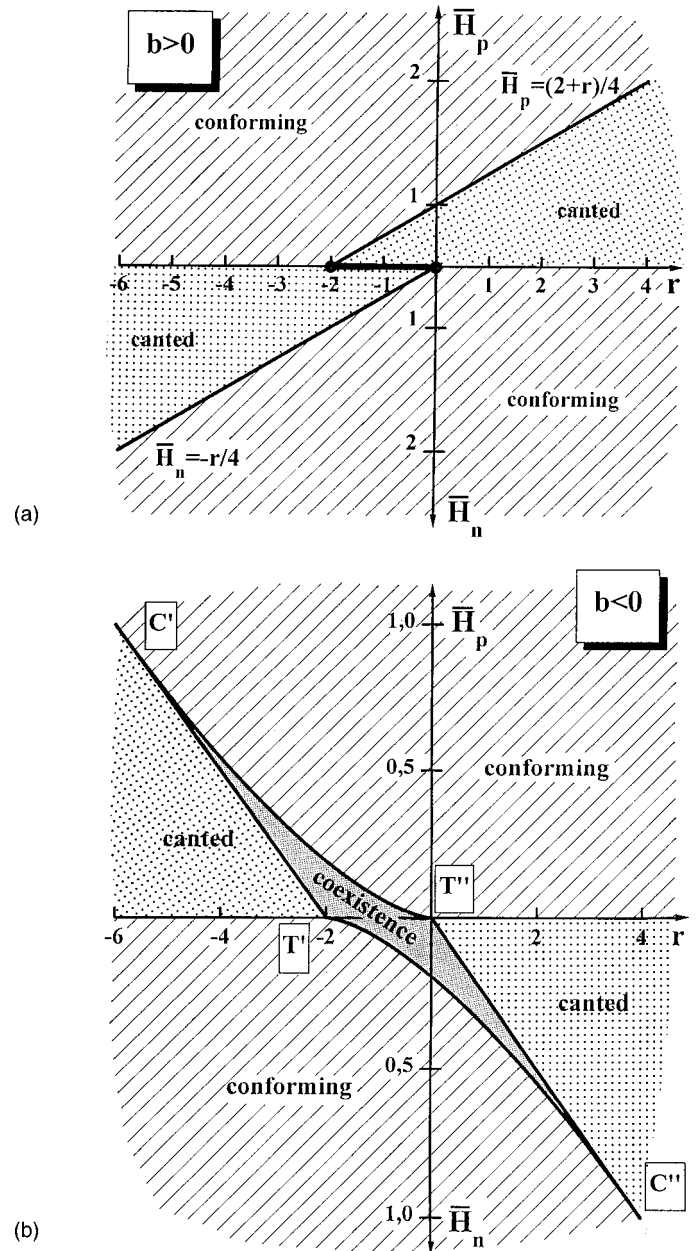


FIG. 4. Phase diagrams in physical terms. Field values are normalized against the critical field  $H_C$  defined by Eq. (23); the abscissa is  $r \equiv a/b$ . Both field configurations are depicted in the same plot (upper half-plane for in-plane, lower half-plane for coaxial field configuration). (a) Positive second-order anisotropy ( $b > 0$ ). Due to the presence of nonzero  $b$ , the simple picture of Fig. 2 ( $b = 0$ ) is substantially modified. As soon as field is applied, only two competitors survive (canted and conforming). With  $b$  positive, only one phase boundary exists for each field configuration. (b) Negative second-order anisotropy ( $b < 0$ ). The possible regions of coexistence of phases are within the curvilinear triangles, whereby the notation of Fig. 3 has been preserved for the most interesting points in the diagram. The extent to which the spontaneous (zero-field) coexistence phenomenon (the segment  $r \in [-2, 0]$  on the abscissa) projects itself onto the problem with field is clearly seen in the offspring curvilinear triangles stemming from this segment.

##### B. Negative higher-order anisotropy ( $b < 0$ )

As mentioned at the beginning of this paper, coexistence of phases in applied field is only possible with a *negative*

second-order anisotropy contribution. This is demonstrated in Fig. 4(b). Once again, the abscissa corresponds to the zero-field case with spontaneous coexistence of coaxial and in-plane phases for  $b < -a/2$ ,  $a > 0$ . The borderlines of stability for the conforming phases are given by  $\bar{H}_n = r/4$  and  $\bar{H}_p = -(2+r)/4$  for the coaxial and in-plane configurations of the field, respectively. The regions of coexistence are enclosed between these two lines, the abscissa, and the line  $\bar{H}_n = (2+r)^{3/2}/\sqrt{216}$  with coaxial field or  $\bar{H}_p = (-r)^{3/2}/\sqrt{216}$  with in-plane field. Analytically, in coaxial field coexistence is found within the region

$$-2 \leq r \leq 0, \quad (24)$$

$$\max(0, r/4) \leq \bar{H}_n \leq (2+r)^{3/2}/\sqrt{216}, \quad (25)$$

while with in-plane field the coexistence region is defined by

$$-2 \leq r \leq 0, \quad (26)$$

$$\max[0, -(2+r)/4] \leq \bar{H}_p \leq (-r)^{3/2}/\sqrt{216}. \quad (27)$$

Altogether, in this representation one can recognize both the form and the extent to which the coexistence phenomenon is held up in the presence of an applied field. The critical values of field and anisotropy beyond which there is no coexistence are given by  $\bar{H} = 1$  and  $-2 \leq r \leq 4$  or  $-6 \leq r \leq 0$  for the coaxial or in-plane configurations, respectively. Note that in order to find coexistence it is only necessary, but not sufficient, to have  $\bar{H} < 1$  or a value of  $r$  within the specified limits. The exact description of the coexistence regions is given by the pairs of equations (24),(25) and (26),(27) which bind together the values of both quantities. The primed letters in Fig. 4(b) denote the same characteristic points as in Fig. 3.

### V. STABILITY DIAGRAMS IN AN ALTERNATIVE REPRESENTATION: SCALING AGAINST THE ZEEMAN AMPLITUDE

Combining the information contained in Figs. 4(a) and 4(b) one can get the complete description of the phase diagram with field for the coaxial or in-plane configurations for any sign of  $b$ . A certain difficulty can be recognized. If the second constant  $b$  approaches zero under the variation of some driving parameter other than the field, the corresponding point in the phase diagrams in Figs. 3 and 4 would tend to infinity.<sup>26,27</sup> A zero point of the second anisotropy constant  $b$  in the ferromagnetic regime is not an abstract possibility as clarified in recent studies of higher-order anisotropies in bulk and thin-film systems. For the bulk, it has been shown that the second anisotropy constant  $b$  may change sign.<sup>28</sup> For ultrathin films, it has been deduced that the surface contribution to  $b$  may have the opposite sign to that of the bulk contribution which means that  $b$  would change sign at some particular thickness of the film<sup>29</sup> (see also Fig. 1 in part II). In an elaborate theoretical microscopic analysis of the temperature dependence of anisotropies of ultrathin films, Jensen has come across values of the microscopic parameters for which both the first and the second overall (phe-

nomenological) anisotropies go through zero at different temperatures.<sup>30</sup>

In the representation of Figs. 3 and 4 it is hard to follow the evolution of the system if  $b$  goes to zero, although it would still be possible to predict where the system would re-emerge after the change of sign.<sup>28</sup> A further difficulty with tracing-down trajectories in the anisotropy space lies with the nonlinear character of the representation even if the field is held fixed. In particular, this means that the variation of the parameter  $r$  would reflect neither the variation of  $a$ , nor that of  $b$ . This would require a further straining of the physical intuition even if the corresponding variation for each of  $a$  and  $b$  is known separately.

On the other hand, in the general analysis of the enthalpy in Sec. II we mentioned that three self-suggesting possible choices of proper units of energy are at hand which opens up the possibility of scaling against  $b$ ,  $a$ , or  $z$ . We have carried out the first case in detail and scaling against  $a$  does not bring new insights. Here we discuss the third possibility, scaling against the amplitude  $z = HM$  of the Zeeman energy. Very generally, it disposes of the difficulties described above. In fact, this representation is an extension of the anisotropy-space representation of the spontaneous (zero-field) case of SRT's and of the related general concept of anisotropy flows.<sup>6,7,31</sup> We develop now the formal relations in this variant which are valid for both bulk and ultrathin systems. Its advantages will be exploited in the following paper in the context of SRT's in thin films.

One defines

$$\alpha = a/z = a/HM, \quad (28)$$

$$\beta = b/z = b/HM. \quad (29)$$

To obtain an exhaustive  $(\alpha, \beta)$  diagram, one has to do but very little. First, the critical lines in Figs. 3 and 4 have to be transformed to the new independent variables  $(\alpha, \beta)$ . Second, the relevant solutions of the minimization problem have to be assigned to the various regions of the representation. For either coaxial or in-plane configurations, a suitable starting point is the respective  $(p, q)$  representation.

#### A. Coaxial field configuration ( $\mathbf{H} \parallel \mathbf{H}_n$ )

With the coaxial configuration ( $\phi = 0$ ), one finds the pair of transforming relations as

$$p = -(1 + \alpha/2\beta), \quad q = -1/4\beta. \quad (30)$$

The inverse transformation is given by

$$\alpha = \frac{(p+1)}{2q}, \quad \beta = -\frac{1}{4q}. \quad (31)$$

The important lines in the  $(p, q)$  diagram of Fig. 3 transform according to the following relations:

$$p + q + 1 = 0 \leftrightarrow \alpha = -\frac{1}{2}, \quad (32)$$

$$p = 0 \leftrightarrow \alpha = -2\beta, \quad (33)$$

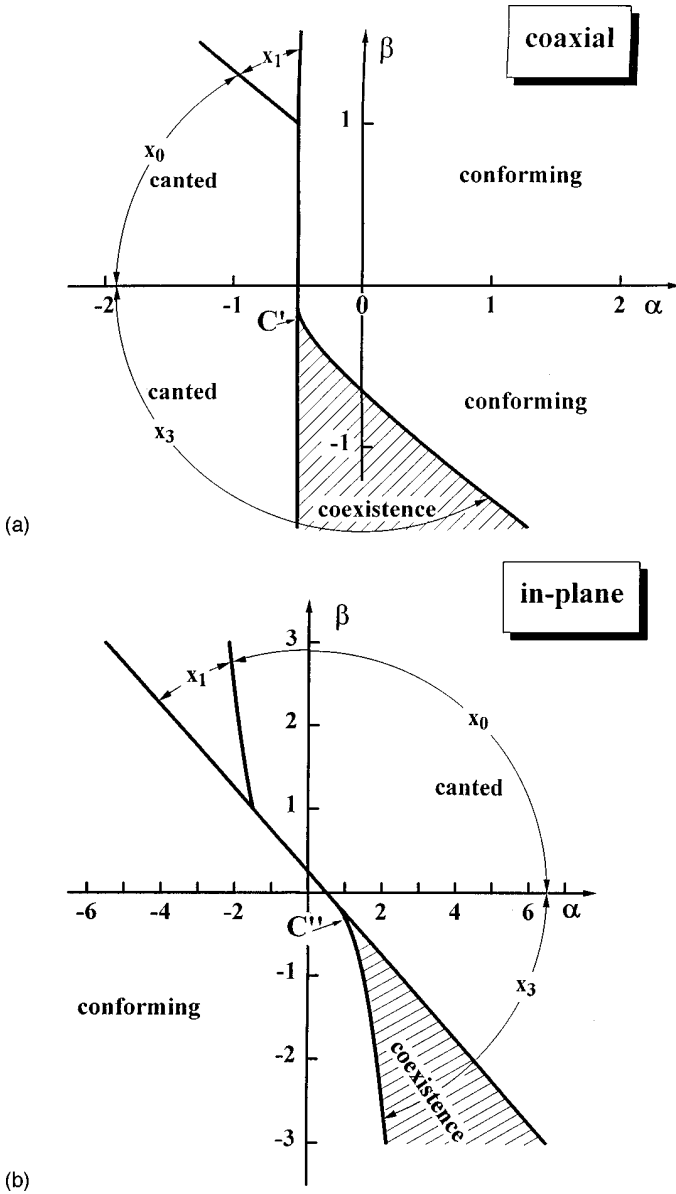


FIG. 5. The  $(\alpha, \beta)$  representation.  $\alpha$  and  $\beta$  are the first and second anisotropy constants scaled against the Zeeman energy. The phase diagrams for coaxial and in-plane field configurations are given in (a) and (b), respectively. The regions of coexistence are shaded. The appropriate solutions of the cubic are indicated; they represent the stable canted-phase solutions.

$$D=0 \leftrightarrow \alpha = -2\beta + \frac{3}{2}\beta^{1/3}. \quad (34)$$

These lines provide the structure arising under the nonlinear mapping of the  $(p, q)$  plane onto the  $(\alpha, \beta)$  plane. The complete result is presented in Fig. 5(a). The most important line is  $\alpha = -1/2$  which arises from the requirement of stability for the conforming phase. The region of coexistence of both conforming and canted phases is shaded in the figure. There, the relevant canted-phase solution is  $x_3$  as given in the Appendix. Remarkably, to the left of the line  $\alpha = -1/2$  in Fig. 5(a), where the canted phase is the one and only stable phase, the relevant canted solution might be any one from among  $x_3$ ,  $x_0$ , and  $x_1$  (see the Appendix). Adding to the list  $x = 1$  ( $\theta = 0$ ) which is the coaxial solution, one finds four

functionally different expressions which have to be eventually considered. It turns out that discontinuous behavior is intimately connected with the coexistence phenomenon in applied field and occurs all the way along the borderline  $\alpha = -2\beta + 3\beta^{1/3}/2$  for  $\alpha > 0$ ,  $\beta < 0$  with the exception of the tricritical point. The location of the tricritical point itself is given by

$$\alpha_c = -\frac{1}{2}, \quad \beta_c = -\frac{1}{8}. \quad (35)$$

### B. In-plane field configuration ( $\mathbf{H} \parallel \mathbf{H}_p$ )

The parameters  $\alpha$  and  $\beta$  are defined in the same way as in Eqs. (28) and (29) by scaling against the Zeeman energy amplitude. The transforming relations now appear even simpler:

$$p = \frac{\alpha}{2\beta}, \quad q = -\frac{1}{4\beta}. \quad (36)$$

The inverse relations are rather obvious. The structure of the  $(\alpha, \beta)$  diagram is obtained by translating the relevant lines according to the following correspondence:

$$p + q + 1 = 0 \leftrightarrow \alpha = \frac{1}{2} - 2\beta, \quad (37)$$

$$p = 0 \leftrightarrow \alpha = 0, \quad (38)$$

$$D = 0 \leftrightarrow \alpha = -\frac{3}{2}\beta^{1/3}. \quad (39)$$

The result of the nonlinear transformation to the anisotropy variables is presented in Fig. 5(b). The line  $\alpha = -2\beta + 1/2$  is the most important one and, as in the previous subsection, stems from the stability condition for the conforming phase. The region of coexistence is shaded, while the coordinates of the critical point are given by

$$\alpha_c = \frac{3}{4}, \quad \beta_c = -\frac{1}{8}. \quad (40)$$

Once again, there is an underlying subgeneric structure, provided by the subregions of the phase diagram where the relevant solutions have a different functional form. Altogether, one encounters the same number of expressions with the coaxial configuration in the preceding subsection. The fourth expression is  $x = 1$  for the conforming phase. We emphasize once again that  $x$  is defined as the normalized component which is collinear with the applied field, hence, here one has  $x = \sin \theta$ . The remarks from the previous subsection about the continuity of the solutions across the borderlines apply here as well.

As mentioned earlier, each of the possible presentations offers some advantages. It is obvious already here that, so far as the coexistence region is concerned, the  $(\alpha, \beta)$  transformation has blown up the corresponding domain in the parameter space considerably, thus making it suitable for further quantitative predictions based on graphical analysis. As a disadvantage, one cannot “observe” the zero-field case in this diagram, since  $H \rightarrow 0$  implies that both  $|\alpha|$  and  $|\beta|$  tend



to infinity. Hence, the trajectories tend to infinity along the appropriate asymptote specified by the particular experimental conditions. One thus loses track, diagrammatically at least, of the natural “continuity” extension of the coexistence phenomenon from the zero-field case to the case with an applied magnetic field.

The  $(\alpha, \beta)$  presentation is especially useful in the treatment of SRT's in ultrathin films. Because of its simplicity, such an analysis seems unavoidable in the thin-film context where the number of relevant anisotropy parameters grows significantly. It will be shown in the second part (see next article) that this representation is a natural extension of the anisotropy-flow concept introduced recently and that the thickness-driven trajectories in the anisotropy space are linear.<sup>6,7,31</sup> This presentation then provides the basis for the unified analysis of facts which otherwise appear as strongly system dependent and disconnected from each other.

## VI. DISCUSSION AND CONCLUSIONS

The analysis provided above is rather general and applicable to both bulk and thin-film systems exhibiting SRT's in the presence of applied magnetic field. One of the important issues has been to show that no conceptual barrier exists between the phenomenological treatments of bulk and thin-film systems. Even if one addresses bulk SRT's only, the analysis provides insights and a compact exhaustive treatment which, to our knowledge, is not available in the literature. We have elaborated three representations for the analysis of the reorientation transition. In all of these, the most important feature is the extinction of the third (nonconforming) phase known from the zero-field case and the existence of a restricted region of coexistence of the remaining two competing phases, the canted and conforming ones. The treatment is carried out for both coaxial and in-plane field configurations. Emphasis was laid on handling a situation where the field is held fixed and the SRT is induced by variation of some other driving parameter. Thus, field-induced magnetization processes are not in the focus, since they have been given enough attention and since we are mainly interested in providing a basis for a unified treatment of SRT's in ultrathin films. Still, all the results can be utilized for discussing magnetization processes as well.

The analytically most natural representation is the  $(p, q)$  representation. It is also the *source* representation, since the more physical ones are derived from it by mere identification of the relevant variables, i.e., practically by means of formal nonlinear substitutions (mappings) whereby a certain particularization is unavoidable if one is to describe correctly the effect of the signs of the anisotropy constants. The structure of the  $(p, q)$  diagram, and hence of those deriving from it, is determined by stability analysis of the allowed phases. In both field configurations, these are a conforming phase (magnetization aligned with the applied field) and a canted phase (magnetization askew to the field). It must be emphasized here that although the canted phase appears as a monolithic piece in all of the diagrams, this is in fact a *nonhomogeneous phase* in the sense that the canting angle varies in different portions of the diagram. Moreover, for a particular trajectory of the system in the corresponding space this angle will vary along the trajectory.<sup>32</sup> Should sufficient information

on the system in question be available, one can deduce from this type of analysis the magnetization profiles along any specified evolution (trajectory) in the anisotropy space. For instance, one can describe the magnetization profile which would be seen on a vertically or horizontally magnetized ultrathin ferromagnetic wedge in a constant external field or one can describe the canting angle in a bulk anisotropic ferromagnet in the presence of field as has previously been done for the spontaneous SRT in bulk systems. This point will be elaborated in the following article.

We have emphasized the advantages and the shortcomings which go together with each of the different representations with the understanding that it is the whole set of distinct representations that adds up to an exhaustive description. As an important example, one cannot treat the zero-field SRT in the  $(\alpha, \beta)$  representation, since the point corresponding to the zero-field case is at infinity; however, it is precisely in this representation that the suitable linear trajectories for the thickness-driven SRT's in ultrathin films are recovered with field as well.

A very important application of the present general formalism is the study of SRT's *within the film plane*, which have already been detected.<sup>33–36</sup> In fact, only minute adjustments are necessary to apply the whole analysis in this paper to such in-plane reorientations in external field applied at different angles within the easy plane. More generally, regardless of the particular crystallographic symmetry, our study is immediately applicable to all cases of bulk and thin-film processes of rotation of  $M$  in an applied field, in the course of which  $M$  remains within a given plane.

We hope that the diagrams presented here are useful tools in preserving the overview and choosing the correct “working point” or experimental conditions for all techniques which exploit the effect of an applied field for studying SRT's or, more generally, anisotropy behavior in uniaxial bulk and thin-film systems. Outstanding among these are the ferromagnetic resonance,<sup>37</sup> Brillouin light scattering,<sup>38</sup> the torque oscillation magnetometry,<sup>39</sup> and the magneto-optic Kerr effect.<sup>40</sup>

## ACKNOWLEDGMENTS

Expert technical assistance by A. Kroder is gratefully acknowledged. Y.M. acknowledges the support of the Max Planck Society and participation in Contract No. NSF  $\Phi$ 560 (Sofia).

## APPENDIX

Here we present concisely the required information about the solutions of a general cubic equation.<sup>25</sup> Given that the equation has been transformed to the form  $x^3 + px + q = 0$ , the number of real solutions depends on the sign of the quantity  $D = p^3/27 + q^2/4$ .

For  $D \leq 0$ , the cubic has three real roots which are suitably cast in a trigonometric form:<sup>41</sup>

$$x_k = -2R \cos[\Phi/3 + 2(k-1)\pi/3], \quad k = 1, 2, 3, \quad (\text{A1})$$

where  $R = \text{sgn}(q) \sqrt{|p|/3}$  and  $\Phi = \arccos(q/2R^3)$ .

For  $D > 0$ , there is a unique real solution, whereby for  $p < 0$  the solution is of the form

$$x_{\text{ch}} = -2R \cosh(\Phi_{\text{ch}}/3) \quad (p < 0), \quad (\text{A2})$$

with  $\Phi_{\text{ch}} = \text{arccosh}(q/2R^3)$ , while for  $p > 0$  the unique solution is

$$x_{\text{sh}} = -2R \sinh(\Phi_{\text{sh}}/3) \quad (p > 0), \quad (\text{A3})$$

with  $\Phi_{\text{sh}} = \text{arcsinh}(q/2R^3)$ .

In our problem, one imposes the additional restrictions that (i) the real root(s) be between zero and unity, and (ii) the stability condition (16) be satisfied. The results are summarized in Fig. 3. The conforming solution (magnetization along the field) is independent of  $p$  and  $q$  and, therefore,

exists everywhere in the  $(p, q)$  plane. For this solution, restrictions depending on  $p$  and  $q$  arise from the stability condition  $d^2 g_A / d\theta^2 \geq 0$  only [cf. Eqs. (8) and (9) in Sec. III A].

The algebraic form of the solutions to the cubic is, of course, completely equivalent to the trigonometric one, but is somewhat clumsy. Still, it might be used to represent the case with  $D > 0$  and either sign of  $p$  compatible with the positivity of  $D$  by a single expression, i.e., instead of  $x_{\text{ch}}$  and  $x_{\text{sh}}$  from above, one might use the algebraic expression for the unique real root:

$$x_0(D > 0) = \left( -\frac{q}{2} + \sqrt{D} \right)^{1/3} + \left( -\frac{q}{2} - \sqrt{D} \right)^{1/3}. \quad (\text{A4})$$

\*On leave from the CPCS Lab, Institute of Solid State Physics, Bulgarian Academy of Sciences, 1784 Sofia, Bulgaria.

<sup>1</sup>L. D. Landau and E. M. Lifshitz, *Electrodynamics of Continuous Media* (Pergamon, Oxford, 1960), Chap. 5.

<sup>2</sup>H. Zijlstra, *Experimental Methods in Magnetism* (North-Holland, Amsterdam, 1967), Chap. 5.

<sup>3</sup>B. D. Cullity, *Introduction to Magnetic Materials* (Addison-Wesley, Reading, 1972), Chaps. 7 and 11.

<sup>4</sup>M. Darby and E. Isaac, *IEEE Trans. Magn.* **10**, 259 (1974); J. M. D. Coey, *Phys. Scr.* **19**, 426 (1987); K. H. J. Buschow, *Rep. Prog. Phys.* **54**, 1123 (1991); J. F. Herbst, *Rev. Mod. Phys.* **63**, 819 (1991); K. Hummler and M. Fähnle, *Phys. Rev. B* **53**, 3272 (1996).

<sup>5</sup>U. Gradmann, in *Handbook of Magnetic Materials*, edited by K. H. J. Buschow (North-Holland, Amsterdam, 1993), Vol. 7, Chap. 1; *Ultrathin Magnetic Structures I*, edited by J. A. C. Bland and B. Heinrich (Springer, Berlin, 1994); M. T. Johnson *et al.*, *Rep. Prog. Phys.* **59**, 1409 (1996); M. Farle *et al.*, *Phys. Rev. B* **55**, 3709 (1997).

<sup>6</sup>Y. Millev and M. Fähnle, *Phys. Rev. B* **52**, 4336 (1995).

<sup>7</sup>Y. Millev and J. Kirschner, *Phys. Rev. B* **54**, 4137 (1996).

<sup>8</sup>D. Krause, *Phys. Status Solidi* **6**, 129 (1964); R. Bozorth, *Phys. Rev.* **50**, 1076 (1936).

<sup>9</sup>J. R. Cullen and E. Callen, *J. Appl. Phys.* **55**, 2426 (1984); *Phys. Rev. B* **30**, 181 (1984); J. R. Cullen, K. B. Hathaway, and A. E. Clark, *J. Appl. Phys.* **81**, 5417 (1997).

<sup>10</sup>L. Néel, *J. Phys. Radium* **15**, 225 (1954).

<sup>11</sup>E. du Tremolet de Lacheisserie, *Phys. Rev. B* **51**, 15 925 (1995).

<sup>12</sup>E. C. Stoner and E. P. Wohlfarth, *Philos. Trans. R. Soc. London, Ser. A* **240**, 599 (1948).

<sup>13</sup>L. G. Onoprienko, *Fiz. Met. Metalloved.* **19**, 481 (1965).

<sup>14</sup>A. I. Mitsek, N. P. Kolmakova, and D. I. Sirota, *Fiz. Met. Metalloved.* **38**, 35 (1974).

<sup>15</sup>I. D. Mayergoyz, *Mathematical Models of Hysteresis* (Springer, New York, 1984).

<sup>16</sup>A. I. Mitsek, N. P. Kolmakova, D. I. Sirota, I. N. Karnaukhov, and A. P. Nedavnii, *Phys. Status Solidi B* **65**, K137 (1974).

<sup>17</sup>G. Asti and F. Bolzoni, *J. Magn. Magn. Mater.* **20**, 29 (1980).

<sup>18</sup>A. I. Mitsek and V. N. Pushkar, *Magnetic Order in Real Crystals* (Naukova Dumka, Kiev, 1978) (in Russian).

<sup>19</sup>G. Asti, in *Ferromagnetic Materials* edited by K. H. J. Buschow and E. Wohlfarth (Elsevier, Amsterdam, 1990), Vol. 3, pp. 398–464.

<sup>20</sup>S. Nieber and H. Kronmüller, *Phys. Status Solidi B* **165**, 503 (1991).

<sup>21</sup>E. du Tremolet de Lacheisserie, *Magnetostriction: Theory and Applications of Magnetoelasticity* (CRC, Boca Raton, FL, 1993).

<sup>22</sup>A physical discussion of the restrictions of this notion is to be found in Ref. 2.

<sup>23</sup>This circumstance is used every time one wants to go over from one convention for the angular-dependent part of  $g_A$  to another (e.g., changing from powers of sines to powers of cosines or vice versa). There is no more to it than fixing the reference zero for  $g_A$  or  $f_A$ .

<sup>24</sup>Ambiguity should not arise with the subscript  $p$  which is used as a notation for the in-plane configuration.

<sup>25</sup>L. N. Bronstein and K. A. Semendjajew, *Mathematical Handbook*, 20th ed. (Nauka, Moscow, 1981), Chap. 2, p. 178; G. Korn and T. Korn, *Mathematical Handbook for Scientists and Engineers*, 2nd ed. (McGraw-Hill, New York, 1968), pp. 17–24.

<sup>26</sup>To avoid misunderstandings, it should be noted that, within the restrictions of the present treatment (only the two major field configurations and only canting between 0 and  $\pi/2$  considered), the evolution of a uniaxially anisotropic system in the  $(p, q)$  space takes place without crossing the ordinate ( $p$ ) axis in Fig. 3. Indeed, at an eventual cross point  $q$  would be zero, but this is only possible if  $H=0$  or if  $b=\infty$ . The first condition implies switching of the field to the opposite direction upon crossing the  $p$ -axis, while the second implies the unphysical situation of a system with an infinite second anisotropy constant.

<sup>27</sup>The case with  $b$  identically zero has already been dealt with above.

<sup>28</sup>Y. Millev and M. Fähnle, *IEEE Trans. Magn.* **32**, 4743 (1996); *J. Magn. Magn. Mater.* **163**, L264 (1996).

<sup>29</sup>H. P. Oepen, M. Speckmann, Y. T. Millev, and J. Kirschner, *Phys. Rev. B* **55**, 2752 (1997); H. P. Oepen, Y. T. Millev, and J. Kirschner, *J. Appl. Phys.* **81**, 5044 (1997).

<sup>30</sup>P. J. Jensen (private communication).

<sup>31</sup>Y. Millev, *IEEE Trans. Magn.* **32**, 4573 (1996).

<sup>32</sup>Trajectories which coincide with isolines of constant magnetization are an exception to this statement.

<sup>33</sup>W. Wulfhekel, S. Knappmann, B. Gehring, and H. P. Oepen, *Phys. Rev. B* **50**, 16 074 (1994); W. Wulfhekel, S. Knappmann, and H. P. Oepen, *J. Magn. Magn. Mater.* **163**, 267 (1996).

<sup>34</sup>D. S. Chuang, C. A. Ballentine, and R. C. O'Handley, *Phys. Rev. B* **49**, 15 084 (1994).

- <sup>35</sup>O. Fruchart, J.-P. Nozieres, and D. Givord, *J. Magn. Magn. Mater.* **165**, 508 (1997).
- <sup>36</sup>M. Brockmann, S. Miethaner, R. Onderka, M. Köhler, F. Himmelhuber, H. Regensburger, F. Bensch, T. Schweinböck, and G. Bayreuther, *J. Appl. Phys.* **81**, 5047 (1997).
- <sup>37</sup>B. Heinrich and J. F. Cochran, *Adv. Phys.* **42**, 523 (1993); B. Heinrich, in *Ultrathin Magnetic Structures II*, edited by J. A. C. Bland and B. Heinrich (Springer, Berlin, 1994); P. Kabos, in *High Frequency Processes in Magnetic Materials*, edited by G. Srinivasan and A. N. Slavin (World Scientific, Singapore, 1995), Chap. 1, pp. 3–55; Z.-Y. Zhang and P. E. Wigen, *ibid.*, Chap. 5, pp. 164–202.
- <sup>38</sup>J. F. Cochran, in *Ultrathin Magnetic Structures II* (Ref. 37); B. Hillebrandts and G. Güntherodt, *ibid.*
- <sup>39</sup>J. H. E. Griffiths and J. R. MacDonald, *J. Sci. Instrum.* **28**, 56 (1951); R. Bergholz and U. Gradmann, *J. Magn. Magn. Mater.* **45**, 389 (1984).
- <sup>40</sup>R. A. Hajjar, F. L. Zhou, and M. Mansuripur, *J. Appl. Phys.* **67**, 5328 (1990); S. T. Purcell, M. T. Johnson, N. W. E. McGee, W. B. Zeper, and W. Hoving, *J. Magn. Magn. Mater.* **113**, 257 (1992); W. Wulfhekel, S. Knappmann, and H. P. Oepen, *J. Appl. Phys.* **79**, 988 (1996).
- <sup>41</sup>Note that negative  $D$  brings about negative  $p$  automatically, hence, three roots can eventually exist only in the third and fourth quadrant of the  $(p, q)$  plane ( $p < 0$ ).